Research Article

Egg shell powder as the Precursor for the Synthesis of nano crystalline Calcium Stannate ($CaSnO_3$) with Orthorhombic Perovskite structure: Exploration on Phase, Morphology and Antioxidant property

Sethumadhavan Sudhaparimala, Arumugam Gnanamani, Asit Baran Mandal*

CSIR - Central Leather Research Institute, Adyar, Chennai 20,Tamil Nadu, India.

Abstract

The present study emphasizes the green method of synthesis of nano crystalline Calcium stannate ($CaSnO_3$) and explores the phase, morphology and biological property of the same. In brief, Calcium stannate was prepared by calcinations of purified tin metal with lime and eggshell powder as the precursor. The analytical studies on structural characterization, phase identification and the surface morphology of the prepared sample concluded the presence of nano crystalline $CaSnO_3$ with orthorhombic perovskite structure. The crystallite size was in the range of 16 – 27 nm range and lattice parameters calculated were well correlated with the JCPDS database. The results of Electro Paramagnetic Resonance study also suggested the presence of non-stoichiometric arrangement of atoms and oxygen deficiency in the crystal lattice and this could be related to the antioxidant property as evidenced by its DPPH• quenching property of the sample. Further, the use of egg shell powder as precursor offered an appreciable porosity as indicated by adsorption isotherms and pore size analysis results and also aided in the effective elimination of metal toxicity in the prepared sample.

***Correspondence**
Dr. Asit Baran Mandal, FASc., FRSC (U.K.),
Director, Central Leather Research Institute,
Adyar, Chennai (Madras) 600020, INDIA.
Tel: +91-44-24910846/24910897/24411630 (Off.)/24421703
Email: abmandal@hotmail.com, abmandal@clri.res.in

Keywords: $CaSnO_3$, Orthorhombic, Perovskite, eggshell powder, nanocrystalline.

Introduction

Materials having perovksite structure are interesting in terms of the principles of solid state chemistry due to their potential applications that arise from their rich crystal chemistry and structure property. Among them, the stannate perovskite structure is a well correlated electronic system which was studied by Mizoguchi *et al* , Zhang *et al* [1, 2] who correlated the band gap with octahedral distortion. According to Azad et al [3], Lu et al [4], many materials of this class have been investigated for their applications as ceramic capacitors, sensors, electrode material in batteries, catalysts, super conductors. Calcium stannate belongs to the family of perovskite materials and Megaw was the first to study the structure of the stannate at room temperature. Among them the perovskite structure of stannates of the form $MSnO_3$ (M= Ca,Sr,Ba) have been widely studied due to their specific applications in ferroelectricity, Piezoelectricity and super conductivity, insulator-metal transition, ionic conduction (Galasso *et al*, Iwahara, Mori *et al* [6],[7],[8]).

With great potential for applications, there are only few reports of the preparation of nano crystalline calcium stannate. Viz :- Solid state ceramic route by Mandal *et al* [9] involving calcinations of metal carbonate and dioxide followed by sintering, Modified wet chemical method by HE Ze *et al* [10] involving the process of annealing the prepared precursor of $CaSn(OH)_6$ at 600 ˚C, Solid state reaction by Novinooz *et al* [11] involving metallic tin and calcium at very high temperatures. But Pffaff *et al* [12] prepared calcium stannate with an orthorhombic structure by solid state reaction between calcium carbonate and tin oxide at a temperature above 1250˚C and the product is being used for electronic and sensor applications.

The structure and the properties of perovskites are greatly affected by precursors used and the factors like particle size, morphology, purity and chemical composition. The current trend on materials research necessitates a green chemical approach and hence, in the present study, an attempt was made to use a biological and economically cheaper source as the precursor

namely, egg shell powder for the preparation of calcium stannate along with metallic tin and lime water. The product thus obtained was subjected to analyses on bulk and surface property to determine the presence of any desirable character (if any) being introduced into the crystal structure. In addition, a preliminary screening for antioxidant property was also carried out to relate the structure with the (re)activity of the product. Such type of study can extend its scope of application in the biological and medical field.

Experimental

Materials and method of preparation

The required materials like metallic tin sheet, Lime, sodium bicarbonate and arsenic trisulphide were obtained from Sigma, India. Egg shell powder was sourced from the nearby poultry. The pure metal was melted in the presence of arsenic trisulphide at the final concentration of 1:1 and the obtained tin powder was ground well with impurities free egg shell powder and then calcined in a crucible in the absence of air at the temperature between 800-1000 ˚C in an oven. The resulting calcium stannate product was allowed to cool in the presence of air to get effloresced and subjected to analyses.

Analyses of Bulk and Surface properties

UV- Visible spectral analysis of the product (in aqueous medium, in methanol, and in dimethlyl sulphoxide), was carried out using Shimadzu UV-2450 UV–visible spectrophotometer in the spectral range of 200–800 nm. For FT-IR spectral analysis, the sample was mixed with KBr (Sigma, India) and the spectrum was recorded using Spectrum one -Perkin-Elmer Co., USA model. All measurements consisted of 500 scans and the plain KBr pellet used as background reference. FT- Raman analysis was performed using FT Raman Bruker RFS 27 with a He: Ne Yag laser with a 100 mW of power (with a excitation wavelength of 1064 nm) in a wavelength range of 50 – 4000 cm^{-1} using a liquid nitrogen cooled Germanium as detector and Rock – Solid interferometer. Perkin-Elmer 5300DV ICP-OES was used for the determination of metallic elements in the product. The percentage composition of C, H, N and S in the sample was determined using Elemental Analyser (Euro Vector model).

Photoluminescence study of the sample was performed using Cary 100 (Varian) Fluorescence spectrophotometer. Thermo gravimetric analysis of the sample was made using TGA Q50 (V20.6 Build 31) and DSC analysis using DSC Q200 (V23.10 Build 79) at nitrogen atmosphere. Powder XRD (PXRD) patterns of the calcined solid sample was recorded using Rigaku Powder X-ray diffractometer with Cu 30KV $^{-1}$15mA and a scan speed of 4° min^{-1} in 2θ range from 10 to 80 degrees with a sampling step of 0.05 deg. EPR spectra of the sample was recorded as a first derivative using Bruker EMX computer controlled spectrometer operating at X-band frequencies (~9.5 GHz) with a rectangular cavity. Brunauer, Emmett and Teller (BET) analysis was carried out to study the surface area and adsorption characteristics. The specific pore volume and distribution of pores in the sample was determined by Barrett - Joyner-Halenda (BJH) analysis.

The surface morphology of the sample was studied using Environmental Scanning Electron Microscope (ESEM) (Hitachi S 4000 voltage of 10Kev). The relative elemental composition of the sample was computed directly with EDX software using ZAF correction. X-ray photoelectron spectroscopic (XPS) analysis was made using Kratos Axis 165 instrument with a dual anode (Mg and Al) and Mg-K_α anode. Morphology and the dimension of the crystal were taken on a JEOL model – 200cx Tunnelling Electron Microscope using an accelerating voltage of 120 kV.

The antioxidant profile of the product was studied using EPR spectroscopy. Sample at 1mg ml^{-1} concentration in ethanol was taken and the DPPH• (Di Phenyl Picryl Hydrazyl free radical) concentration was fixed as 2 mM in ethanol. The sample was added to $DPPH^{\bullet}$ and allowed to remain in equilibrium for 30 minutes. EPR signal of $DPPH^{\bullet}$ was recorded after the equilibrium was reached and the g-value was measured and the free radical equivalent was calculated from the double integrated spectrum. The absorption intensity as obtained from the double integrated spectrum was related to the free radical ($DPPH^{\bullet}$) concentration.

Results and Discussion

The resulting product of preparation Calcium stannate ($CaSnO_3$) was white in colour, alkaline in nature. The representative UV-Visible spectra of the sample in methanol, aqueous medium, and dimethlylsulphoxide, displayed from the bottom in the **Figure 1** showed a λ_{max} 220 - 230 nm in the UV region. There were number of small excitation peaks appearing at different energies in the UV-Visible spectra of the sample and could be reasoned to the presence of different sized nano crystals. Literature reports on UV- Visible spectra are not available for reference. The FTIR spectrum of the prepared calcium stannate sample shown in **Figure 2** displayed peaks at 475(w), 613(w), 665(m), 821(s), 1362(w), 1558(m) cm^{-1}. The metal – oxygen bond became more defined as expected at higher temperatures. The appearance of sharp peak at 821 cm^{-1} may be due to Sn- O matrix as observed by Bos *et al* [13]. The presence of thin intense bands at 665 and 475 cm^{-1} also indicated a smaller short range disorder. The absence of peaks at 1450, 1088, and 850 cm^{-1} indicated the absence of inorganic carbonates based on Nakamato [14]. But Mary Alves *et al* . [15] observed two IR bands at 639 cm^{-1} and 462 cm^{-1} for $CaSnO_3$ and at 893, 1090 and 1420 cm^{-1} due to carbonates when the calcinations

were carried at 700 ˚C. The absence of carbonate peaks in the present study may be attributed to the higher calcinations temperature of the natural source of the precursor, which also contains elements like Fe, Mg, P, K at the micro level.

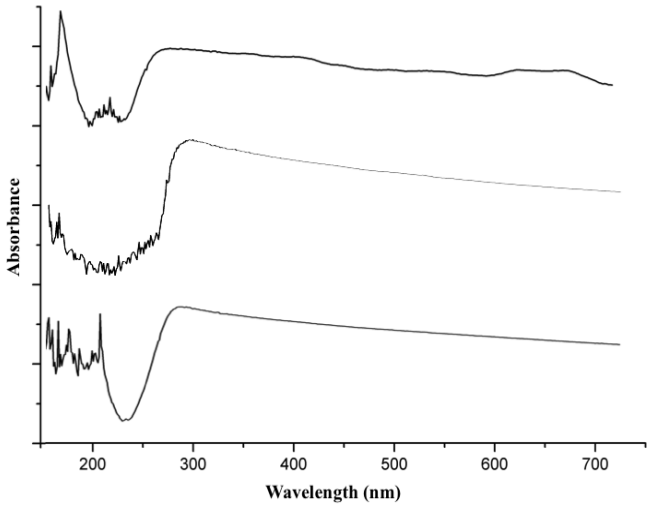

Figure 1 UV-Visible spectrum of nano crystalline, calcium stannate prepared from egg shell powder as the precursor in Methanol, Aqueous medium, and DMSO (viewed from bottom to top in the figure) solvents

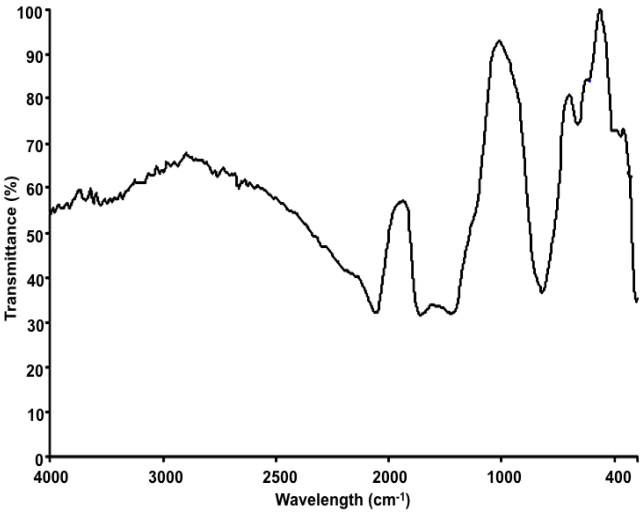

Figure 2 FT-IR spectrum of nano crystalline, calcium stannate prepared from egg shell powder

Figure 3 illustrated FT- Raman spectra of the sample and displayed a strong peak at 780 cm $^{-1}$ due to Sn –O symmetric stretching and weak peak at 1181 cm $^{-1}$, and 2201 cm $^{-1}$, due to N-H stretching. According to Castro *et al* [16], the Raman spectra observed for materials at the excitation wavelength of less than 1064 nm experience dispersive effect and may display many peaks that are not covered by that of 1064 nm. For an orthorhombic $CaSnO_3$, the Raman active modes are given by $T_{Raman} = 7A_g + 5B_{1g} + 7B_{2g} + 5B_{3g}$ which corresponds to four anti symmetric, two symmetric octahedral stretching modes, four bending modes, and six octahedral rotation or tilt modes. The other eight modes are associated for calcium cations. Redfern *et al*. [17] observed Raman modes for $CaSnO_3$ (prepared using synthetic calcium carbonated and metallic tin) at 165, 185, 223, 230, 250, 267, 281, 307, 360, 445, 511 and 702 cm^{-1} at room temperature by using excitation wavelengths of 514.5 and 632 nm. In contrast, in the present study, the Raman shift was observed only at 780 cm^{-1} when excited at wavelength of 1064 nm. The crystalline nature and absence of carbonate given by the Raman study correlated well with the PXRD results. The absence of surface phonon modes and phase transition could also be inferred from the results.

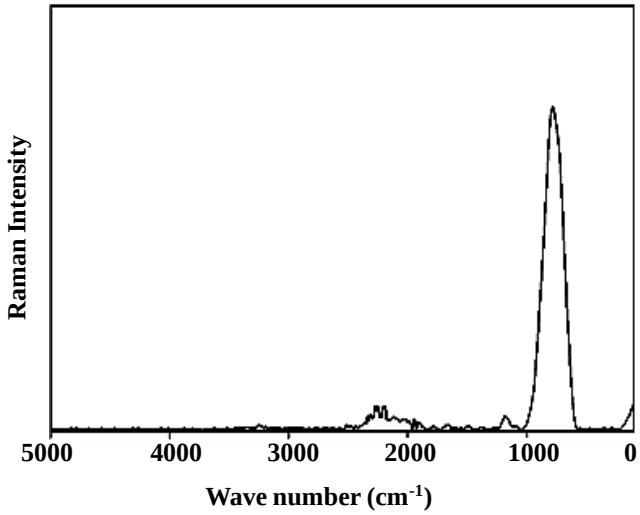

Figure 3 FT-Raman spectrum of nano crystalline calcium stannate prepared from egg shell powder as the precursor

The bulk composition of the uncalcined egg shell powder and the product was determined by ICP-OES (**Table 1**) analysis and a comparison was made. The presence of C, N, S as shown and the absence of H in the product infers the presence of organic moiety, which has been realised in the FTIR peaks at lower intensity. However the exact nature of the organic moiety could not be established with the available spectral data.

From Table 1, it has been found that egg shell powder was the power source of CaO required for the formation of $CaSnO_3$ in the present study. According to Witoon *et al*. [18], egg shell powder converted more of calcium carbonate into CaO than the commercial $CaCO_3$ and the calcined egg shell exhibited small particle size with macroporous volume, which provided higher surface for the reaction of CO_2.

Table 1 Bulk composition of the nano crystalline calcium stannate prepared in comparison with that of the precursor

Sample	Weight percentage of elements										
	Ca	**Mg**	**Fe**	**Na**	**Si**	**Sn**	**S**	**P**	**C**	**N**	**H**
Un calcined eggshell powder	36.66	0.29	0.002	0.01	-	-	-	0.1	-	-	-
Calcium stannate	6.79	BDL	BDL	BDL	BDL	9.39	14.17	BDL	5.3	6.7	Nil

The reactions involved in the processing of the sample can be interpreted in terms of the chemical changes as summarised below:

Initially, tin was purified and the addition of arsenic trisulphide to molten tin removes lead (if present), as sulphide as shown in the following reaction and the As_2O_3 volatilises off:

$$Pb + AsS_3 \rightarrow PbS + As_2O_3 \qquad (1)$$

In the next step, addition of egg shell powder and lime water and calcinations at temperature more than 800 - 1000 ˚C and in the absence of air transforms tin metal to tin oxide. The oxygen can be provided by the carbonates present or by the hydroxide of calcium.

The $Ca(OH)_2$ present in the mixture hydroxylate Sn to form species like $Sn(OH)_4$ which at higher calcinations temperatures undergo the following reaction as given by Giesekke *et al* [19], the most important step in the transformation to tin (IV) oxide:

$$Sn(OH)_4 \rightarrow SnO_2 + H_2O \qquad (2)$$

During this stage, three types of reactions take place,

$$CaCO_3\,(\text{egg shell powder}) \rightarrow CaO + CO_2\,(g) \quad \text{at } 500 - 850\ ^\circ C \qquad (3)$$

According to Gilchrist *et al*. [20] calcinations of synthetic $CaCO_3$ takes place when $\Delta G^0 = 0$ and this happens when T (temperature) is around 848 ˚C. But in the present study, the transformation of calcium carbonate to calcium oxide starts even at 500 °C and the difference in melting point observed in the present study might be due to the origin of calcium carbonate, that is, the egg shell powder, the biological origin acting as a source. But an active, porous CaO with fewer impurities was obtained in the present study also.

During the processing, addition of lime water also maintains the amount of CaO, which is required for the formation of $CaSnO_3$ as shown in the following reactions:

$$Ca(OH)_2\,(s) + CO_2(g) \rightarrow CaCO_3 + H_2 \qquad (4)$$

In the final reaction, tin (IV) oxide reacts with Calcium oxide and transformed to calcium stannate as shown below:

$$SnO_2 + CaO \rightarrow CaSnO_3 \qquad (5)$$

The above series of reactions indicated that there was a continuous buffering of CaO for the formation of calcium stannate

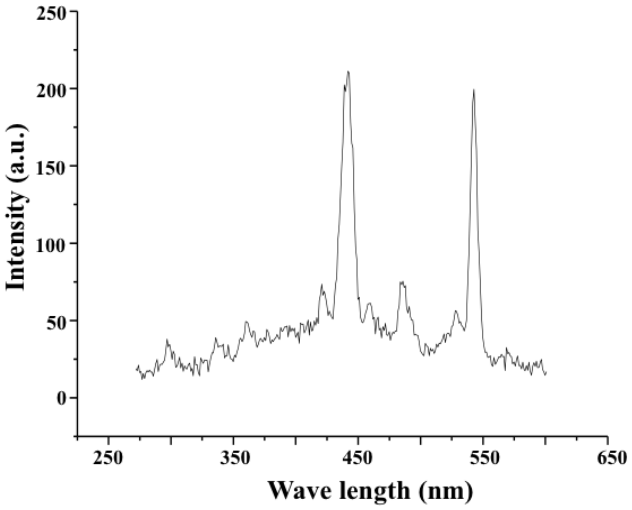

Figure 4 Photoluminescence spectrum of nano crystalline calcium stannate prepared from egg shell powder as the precursor

The photoluminescence study of the product sample dispersed in phosphate buffer of neutral pH 6.9 displayed peaks at 441 and 542 nm when excited at 295 nm (**Figure 4**). According to Van Heusden *et al*. [21], the peak at 540 nm is due to the strongly ionised oxygen state. The photoluminescence property of bulk SnO_2 showed peaks at 440 and 543 nm. The presence of Sn^{4+} ion in the crystal lattice was confirmed from these values.

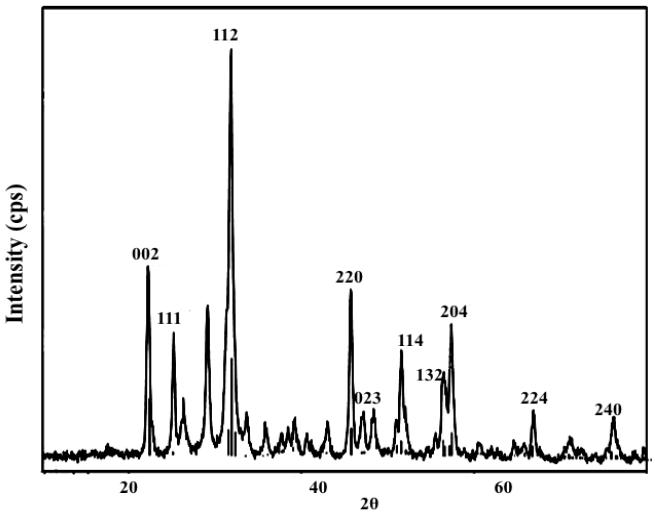

Figure 5 Powder X- ray diffractogram of nano crystalline calcium stannate prepared from egg shell powder as the precursor

Figure 5 depicted the PXRD patterns of the prepared sample and the peaks observed were matched well with that of orthorhombic perovskite structure of $CaSnO_3$ (JCPDS 77- 1797**).** The small intensity peak at 26.3 can be ascribed to tetragonal tin oxide (JCPDS 77-0450). There were also small intensity peaks, which could be correlated with organic peaks of low intensity observed in the FTIR spectrum. But Singh *et al*. [22] also observed the same type of results for mercury based traditional drug Ras- Sindoor and the organic peaks in FTIR were attributed to formation of organo metallic complexes, which would have sustained high calcinations steps. The result also correlated well with the TEM images. However, the sharp PXRD patterns clearly indicated the crystallinity of the sample.

The peaks corresponding to carbonate species (2θ = 26.7, 32.8, 51.4 (JCPDS 84 - 1778**)** were absent in PXRD spectra which correlated well with the FT-IR results.. During the preparation of the sample, there was absence of secondary phase due to calcium carbonate as observed for the synthetic preparations. The absence of inorganic carbonate and the presence of higher covalent character of Ca (Ca^{2+}) facilitated the crystallisation of samples during higher temperature of calcinations which was also observed by Green *et al* [23]. There was no shift of PXRD peaks of the sample in comparison with the JCPDS value as the weight percentage of the other elements shown by EDX and ICP-OES were too low to be detected in the crystal lattice. The percentage of Ca observed from ICP-OES analysis (6.79%), correlated well with the presence of calcium detected in the crystal lattice of tin oxide.

The lattice parameters of the sample were compared with that of various reported values and were summarized in **Table 2**.

Table 2 Lattice parameters of the nano crystalline calcium stannate prepared from egg shell powder as the precursor in comparison with the literature report

Reference	Lattice parameters in ang.			Lattice volume in ang.	Space group
	a	b	c		
Acta Cryst. (1986). JCPDS 771797 [24]	5.532(2)	5.681(2)	7.906(2)	248.46(1)	Pbnm (62)
Zhao *et al* 2004 [25]	5.5142(2)	5.6634(2)	7.8816(17)	246.13(5)	Pbnm (62)
Mary *et al*. 2007 [15]	5.524	5.665	7.940	248.47(3)	Pbnm (62)
Mount Stevans *et al*. 2007 [26]	5.4099	5.5887	7.7459	234.19(1)	Pbnm (62)
Current study	5.532(3)	5.668(2)	7.924(3)	248.48(3)	Pbnm (62)

The lattice parameters and the lattice volume showed a similarity with the reported values, which indicated the absence of doping of any of the elements (Results from ICP – OES analysis) into the crystal lattice of calcium stannate. Also, the lattice volume of the sample was lower than the reported values indicating the absence of secondary phase of Ca_2SnO_4 and smaller long range disorder with less defective structures, which is contrary to what is usually observed when a carbonate is used as a precursor [15]. It may be due to the complete removal of metal carbonate as evident from the XRD, FTIR and TGA results of the study.

The crystallite size of each sample in the most intense planes were calculated by Debye Sherrer equation, as given below after quadratic smoothening followed by Lorentian curve fitting of the peaks.

$$D = \frac{K\lambda}{\beta \cos\theta}$$

Where, *K* is the shape factor, λ is the x-ray wavelength (1.5406 Å), β is the line broadening at half the maximum intensity (FWHM) in radians, and θ is the Bragg angle D is the mean size of the ordered (crystalline) domains, which may be smaller or equal to the grain size as given by Patterson[27].

The crystallite size was calculated in the intense planes and found to vary between 16 and 27 nm. The presence of nanocrystallites could also be inferred from the broadening of the peaks. The peak at 2θ = 79.7 due to CaO overlapped with the 305 plane of orthorhombic $CaSnO_3$.

Novinooz *et al*. [11] used the solid state reaction to prepare $CaSnO_3$, Ca_2SnO_4 through different weight ratios of Sn:Ca to obtain nanocrystalline powders at ambient temperatures in air to give nanocrystals with narrow size distribution. Larger grains were formed due higher temperature and several repetitions of annealing and mixing steps [9]. In the present study, moderate temperature and gradual cooling procedures provided nanocrystallites of $CaSnO_3$.

The EPR spectra of the sample measured at room temperature shown in **Figure 6** demonstrates a scattering of 'g' parallel values indicating the distribution of sizes of nano crystallites and the non-stoichiometry of the crystal lattice. The '$g_{\parallel}$' value was found to be varying between 2.57 and 2.58 and $g_{\perp}$ was found to be 2.018 and then $g_{ave.}$ was found to be 2.2.

The EPR spectra obtained under liquid nitrogen temperature showed small kinks at g = 4.228, which may be due to the presence of traces of iron as detected by ICP-OES analysis.

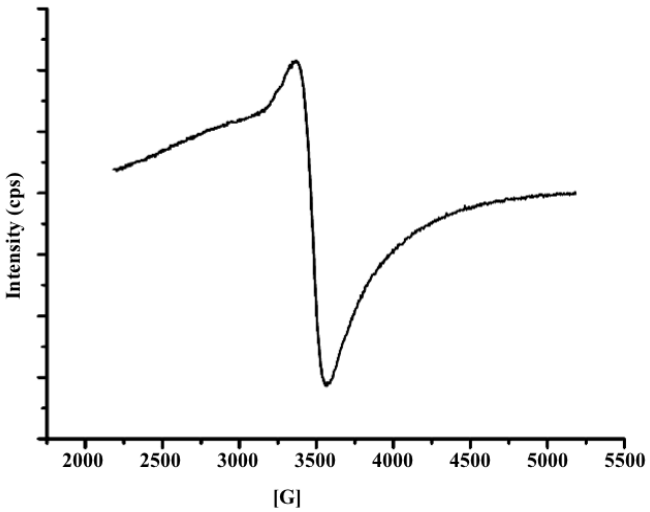

Figure 6 EPR spectrum of nano crystalline, calcium stannate prepared from eggshell powder as the precursor

Table 3 Thermal analysis of the precursor (Egg shell powder) and nano crystalline calcium stannate prepared from egg shell powder

Sample	Step	T_{range} (°C)	% Mass loss	DTG $_{peak}$/°C
Precursor (egg shell powder)	1	50-290	1.5	45, 101, 128, 230
	2	291-652	3	
	3	653-681	1.5	
	4	682-685	2.8	
	5	686-790	1.7	
Product (Calcium stannate)	1	50-109	1	86
	2	110-391	3.4	200
	3	392-594	2	387, 402
	4	595-711	9.6	695, 711
	5	712-790	1	

Table 3 represented the thermal analysis of the precursor (Egg shell powder) and the product of the present study, calcium stannate. It has been observed that there was not huge loss in the mass of the samples upto 750 °C (Fig. 3b) suggesting the absence of carbonate. The trend was different from that reported by Mary Alves *et al*. [15] using synthetic calcium carbonate as the precursor. According to Choi *et al*. [28], the calcined egg shell powder is more porous when calcined around 800 ˚C due to the removal of CO_2 and according to Park *et al*. [29], calcined egg shell powder can remove Cd, Cr, Pb efficiently. These two factors played an important role in the removal of toxic elements from the prepared sample.

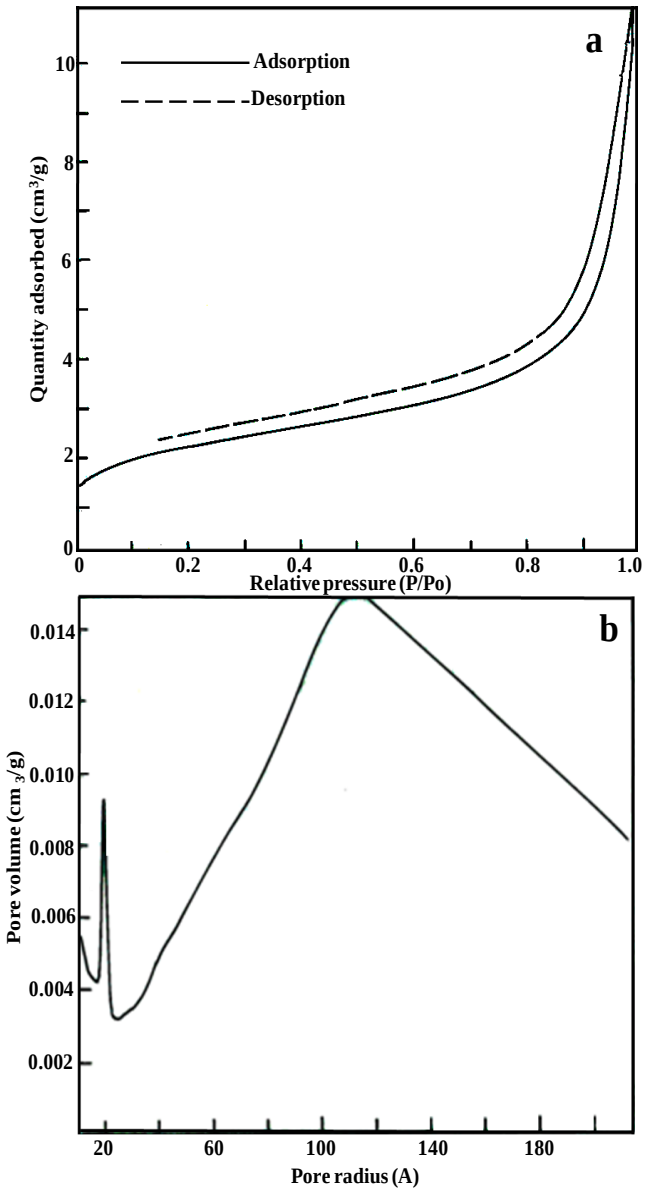

Figure 7 (a & b) BET isotherms & BJH pore size analysis of nano crystalline, calcium stannate from eggshell powder as the precursor

The results of the BET study and BJH pore distribution of the sample were shown in **Figure 7a and Figure 7b** respectively**.** The BET study of the sample gave Type II isotherm and BET surface area was calculated as 7.8 $m^2 g^{-1}$ compared to 8.52 $m^2 g^{-1}$ for the bulk tin oxide and there was absence of hysteresis in the isotherm. According to Ciambelli *et al* [30], perovskites generally have surface area less than 10 $m^2 g^{-1}$ based on the method of preparation and in the present study the grain size was found to be 109.75nm. But, Pfaff *et al*. [12] obtained a surface area 10 $m^2 g^{-1}$ and mean particle size of 0.11 micrometer with a strong agglomeration and grain growth for the calcinations carried out at a temperature of 1000 ˚C for 8 h by the peroxide route.

The BJH pore distribution curve showed two peaks at 20 Å and a narrow range of 110 and 118 Å indicating two types of pores. This can be correlated with the TEM picture showing the coexistence of crystalline CaO and SnO_2 lattices. The small pores also explained about the presence of agglomerates leading to lower adsorption of the drug samples. The cumulative pore volume was 0.015 $cm^3 g^{-1}$ and the cumulative pore area was found to be 5.38(4) $m^2 g^{-1}$.

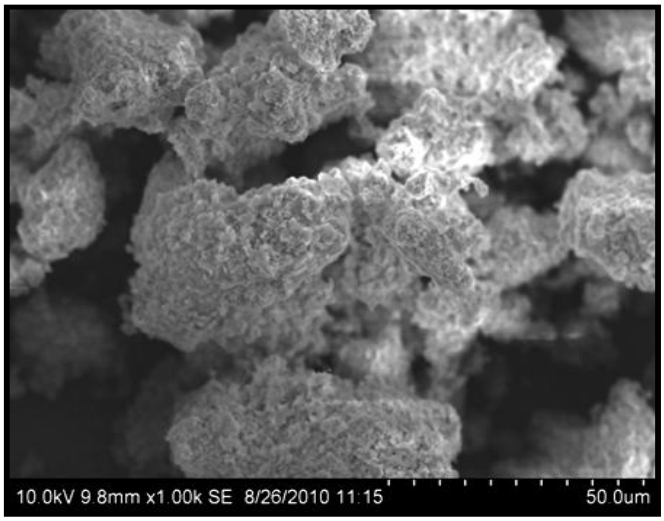

Figure 8 SEM image of nano crystalline calcium stannate prepared from egg shell powder as the precursor

Figure 8 illustrated the SEM image of the sample which showed the formation of spherical grains with agglomeration of grains with large number of pores, as evidenced from the BJH pore analysis. The big agglomerates with connected pores can be related with the porous nature of the egg shell powder, which was used as the precursor in the present study. This type of small crystallite size with granular connectivity is a desired feature for the bioavailability of the sample in the human system. The agglomeration of the particles was evident as the grain size was greater than the crystallite size calculated by the Scherer method. This can be due to the higher calcinations temperature and the presence of oxide of Fe, C shown by the XPS results.

The non-stoichiometry was evident from the percentage of Ca, Sn and O so as to account for the lattice of $CaSnO_3$. The elements detected in the ICP-OES were also accounted in EDX reports attached to SEM.

The TEM images of the sample as given in the **Figure 9a** showed the presence of irregular shaped rods and nanometric sized particles. The rods may be due to CaO and other shaped agglomerates may be due to the presence of Sn, O and or may be organo –metallic complexes which would have survived high calcinations temperatures. The presence of organo-metallic complexes may act as a carrier for the calcium stannate as reported by Singh *et al*.[22] The diffraction rings (**Figure 9b**) observed was due to CaO, which is correlated with the crystalline structure. The EDAX values (not given in the present report) corresponding to the images matched well with the surface composition indicated by XPS results. The bioavailability of calcium stannate sample can be well understood from the surface morphology. It also suggested its application as a promising sensor.

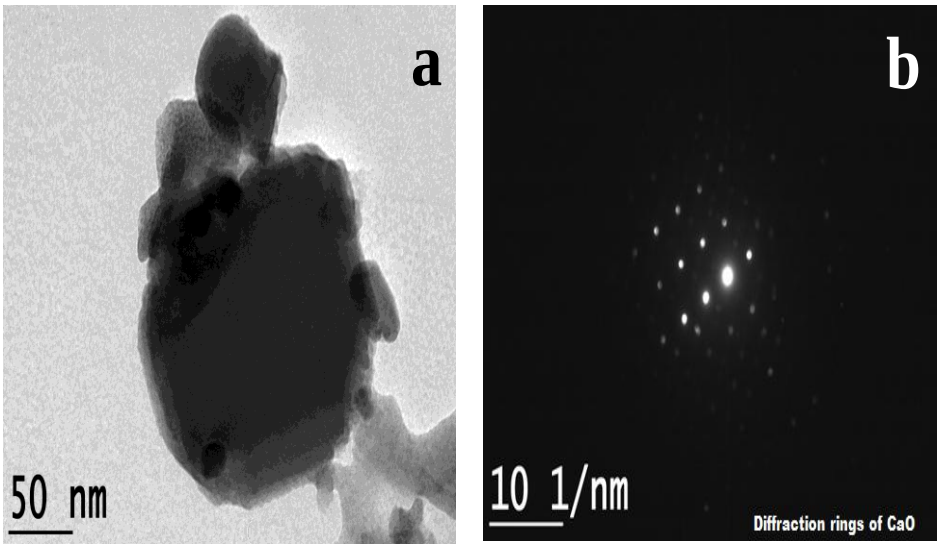

Figure 9 TEM image of nanocrystalline calcium stannate prepared from egg shell powder as the precursor

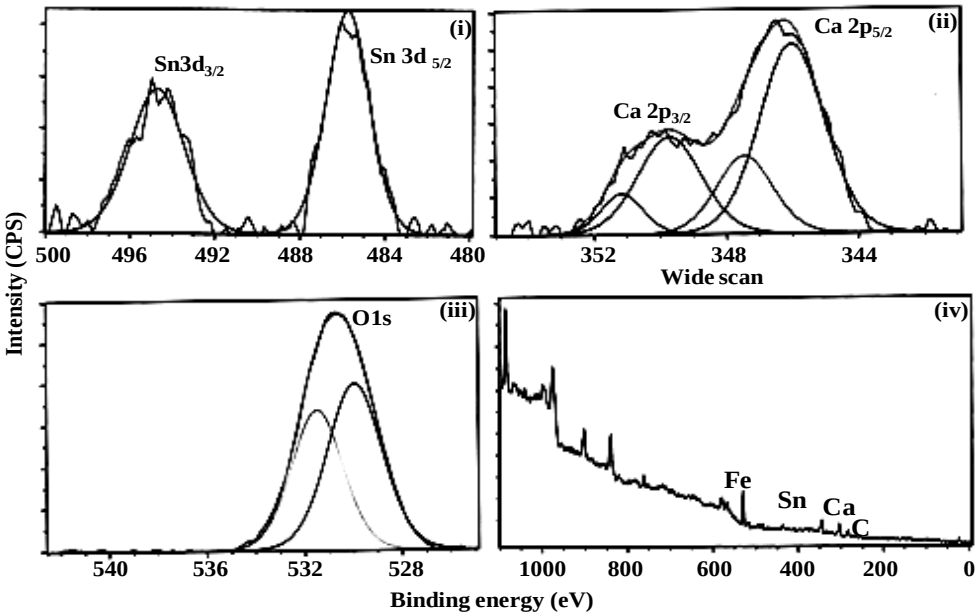

Figure 10 XPS Spectrum of nano crystalline, calcium stannate prepared from egg shell powder as the precursor or i. Binding energy curve of Sn 3d $_{3/2}$ & Sn 3d $_{5/2}$; ii.Binding energy curve of Ca 2p $_{3/2}$ & Ca 2p $_{5/2}$; iii. O(1s) and (iv) wide scan spectra of calcium stannate

Table 4 Comparison of Core binding energy levels of Sn, Ca and O_2 from XPS analysis for the nanocrystalline, calcium stannate with the available reports.

Sample	Element	Binding energy (eV)	Reference
$CaSnO_3$ (Calcium stannate)	$Sn(3d_{5/2} : 3d_{3/2})$	485.7 : 494.1 (Δ=8.4)	Sharma *et al* 2005 [34]
$CaSnO_3$	$Sn(3d_{5/2} : 3d_{3/2})$	485.7 : 494.7 (Δ= 9.0)	present study
Bulk SnO_2(tin IVoxide)	$Sn(3d_{5/2} : 3d_{3/2})$	486.6 : 495.0 (Δ=9.4)	present study
$CaSnO_3$	O(1s)	529.3 and 531.4	Sharma *et al* 2005[34]
$CaSnO_3$	O(1s)	529.9 and 531.5	present study
Bulk SnO_2	O(1s)	530.8 and 531.9	present study
$CaSnO_3$	$Ca(2p_{3/2} : 2p_{1/2})$	346.2 : 349.7 (Δ=3.5)	Sharma *et al* 2005[34]
$CaSnO_3$	$Ca(2p_{3/2} : 2p_{1/2})$	346 .0 : 349.7(Δ=3.7)	present study

X-ray Photoelectron Spectroscopy (XPS) is a powerful and non- destructive route for the determination of valence state/oxidation state of the elements at the surface. So far there are a very few specific reports available on the XPS of $CaSnO_3$ and **Table 4** illustrated the comparisons on core binding energy levels of Sn, Ca, O_2 with the available reports. **Figure 10(i-iv)** showed the XPS core level spectra of the Sn 3d, O(1s), Ca(2p) regions and wide scan spectra. Base line and curve fitting of the raw data were also shown in the same figure. The broad and asymmetric peak for O (1s) at 531.5 and 529.9 eV indicated the presence of two types of oxygen namely, lattice oxygen and adsorbed oxygen respectively. The same type of asymmetric peak was obtained for other perovskite based oxide compounds by Yokoi *et al* [31]. The lower binding energy of the peak in the sample compared to bulk tin oxide indicated the presence of more active oxygen species as observed by Machida *et al* [32] and hence the existence of CaO and SnO_2 without their individual identity.

Also, the area under the curve for adsorbed oxygen was more compared to that in the bulk tin oxide and, it can be inferred that the other elements identified by ICP-OES studies were able to diffuse to the surface in the form of oxides. This type of perovskite structure has a great capability of releasing significant amounts of lattice oxygen at low temperatures, which plays a very important role in its catalytic activity according to Buciuman et al [33].

From **Table 4,** we find that the Ca(2p),O(1s) and Sn(3d) binding energy of the sample correlated fairly well with the reported value of Sharma *et al*. [34] and the difference being in the range of 0.2 to 0.6 eV, the nature of the precursor, calcinations and annealing temperatures would have played a role. Also the tetra valency of tin with adsorbed oxygen and a dual valency of Ca in the sample were confirmed by the XPS spectra.

Antioxidant profile using EPR spectra

For antioxidant profiling of the sample, the free radical quenching behaviour was assessed using EPR spectroscopy. The free radical equivalent of $DPPH^{\bullet}$ of the sample was calculated. In **Figure 11,** the curve (i) represents EPR spectrum of $DPPH^{\bullet}$ while (ii) represents the EPR spectrum of $DPPH^{\bullet}$ after being quenched by the drug sample. The free radical equivalent of $DPPH^{\bullet}$ per mg of the sample was calculated and found to be equivalent to 0.721.

There are reports of similar preparation of calcium salt of tin oxide in the Indian System of Medicine which finds application in the treatment of several diseases [35]. The antioxidant screening report of the present study can provide gives a clue to such applications.

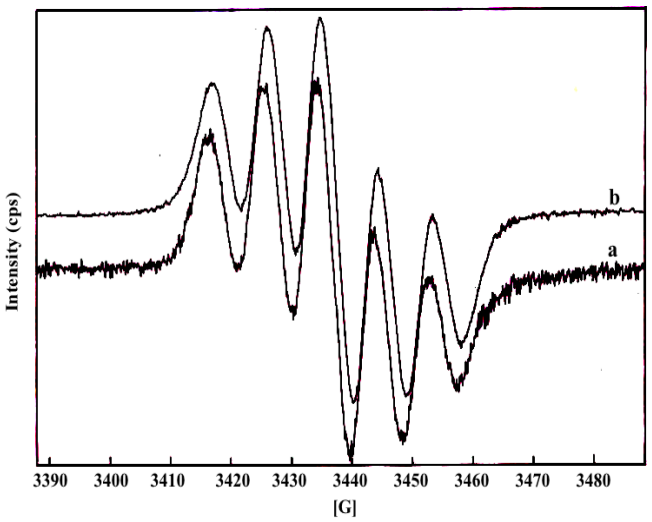

Figure 11 DPPH• quenching by the nanocrystalline, calcium stannate prepared from egg shell powder as the precursor
b. EPR signal of DPPH•- Before quenching
a. EPR signal of DPPH•- After quenching

Conclusion

The above study provided a green and cost effective approach to the preparation of nano crystalline $CaSnO_3$ (Calcium stannate) with an orthorhombic perovskite structure without passing through any secondary phase of carbonate and $CaSn_2O_4$. The study also provided a new dimension to the application of orthorhombic calcium stannate, which has not been explored so far. Also, the properties of the prepared sample matched well with the reported results of other synthetically prepared samples. The bulk property, surface composition and morphology of the prepared sample as determined by various analytical techniques discussed above indicated the non-stoichiometry arising due to oxygen deficiency. It also gives a clue for its anti oxidant property which can be extended further for its medicinal applications in the field of Arithritis and Cancer. The overall study provided a new direction in the synthesis, characterization, and application of calcium stannate with perovskite structure.

Competing interests

The authors declare that they have no competing interests

Acknowledgement

The author S.Sudhaparimala is thankful to the University Grants Commission, Govt. of India and Ethiraj College for Women, Chennai, Tamil Nadu, for the award of UGC-FIP fellowship under the XI Plan. The author is also grateful to IIT Madras for providing the instrumental facilities.

References

[1] H. Mizoguchi and P.M.Woodward, *Chem.Mater*., 2004,16, 5233-5248.
[2] W.F. Zhang, J. Tang, and J. Ye. *Chem. Phys. Lett.*, 2006, 418, 174-178.
[3] A.M. Azad, L.L.W. Shyan, and P.T. Yen, *J Alloys Compd*., 1999, 282, 109–124.
[4] Z. Lu, J. Liu, Y. Tang and W. Li, *Inorg Chem Commun*., 2004, 7, 731-733.
[5] H.D.Megaw, *Proc. Phys. Soc*. London., 1946, 58, 133.
[6] F.S.Galasso , *Perovkites and High T_c super conductors*, Gorden and Breach Science Publishers: London; 1990.
[7] H. Iwahara , *Sol Stat. Ionics*., 1992, 52(1-3) , 99-104.
[8] T. Mori , K. Aoki , N. Kaegashira , and T. Shishido , *Mater. Lett*., 2000, 42, 387.
[9] K.D. Mandal , M. S. Sastry, and O. Parkash, *J Mater Sci Lett*., 1995,14(17), 1412-1413.
[10] Ze- qiang He, Xin- hai Li, En-hui Liu, Zhao-hui Hou, Ling-feng Deng and Chuan-yue Hu, J Cent. South Uni. Tech., 2003, 10, 3, 195 – 197.
[11] Novinooz , Abdoljaved, Sarabadani, and Parvin , Iranian *J Chem and Chem. Eng*., 2009, 28(2),113.
[12] G.Pfaff, *Mater. Sci. & Eng*., 1995, B (33), 156-161.
[13] A. Bos, and J.S.Ogden, *J Phy. Chem*., 1973, 77 (12), 1513-1519.
[14] Nakamato, *Infrared spectra and Raman spectra of Inorganic and Coordination Compounds*, John Wiley & Sons New York, 1986.
[15] Mary C.F.Alves, Soraia C. Souza, S.J.G. Lima, E. Longo, A.G.Souza, Ieda M.G. Santos, *J.Therm. Anal. & Calor*., 2007, 87(3), 763-766.
[16] K.Castro, M. Perez-Alonso, M.D. Rodriguez-Laso, L.A. Fernandez, and J.M. Madariaga, *(e-VISART database), Anal. Bioanal. Chem*., 2005, 382, 248-258.
[17] S.A.T.Redfern, C.J. Chen, J.Kung, O.Chaix-Pluchery, J. Kreisel, E.K.H. Salje, *J Phys-Condens Mat.*, 2011, 23, 425401.
[18] T. Witoon, *Cer. Int*., 2011, 37 (8), 3291-3298.
[19] E.W.Giesekke, H.S. Gutowsky, P. Kirkov, H.A. Laitinen, *Inorg. Chem*., 1967, 6, 1294-1297.
[20] J.D. Gilchrist, *Extraction metallurgy*, 3rd edition, Elsevier Science and technology, United Kingdom; ISBN: 0080366120, 1989.
[21] K. Vanheusden, W.L. Warren, C.H. Seager, D.R. Tallant, J.A.. Voigt, B.E. Gnade, 1996, *J App Phy*., 1996, 79, 7983-7990.

[22] S.K. Singh , A.C, Rai. D.K, Rai S.B. Rai, *IJTK*., 2009, 8, 346-351.
[23] M.A.Green, K. Prassides, P. Day, P, and D.A. Neumann, *Int J Inorg Mater*., 2000, 2(1), 35-41.
[24] A.Vegas, M. Vallet- Regi, J.M. Gonzalez- Calbet and M.A. Alario- Franco, *Acta Cryst*., 1986, Vol. B (42**)**, 167-172.
[25] Zhouguang Lu, Junfeng Liu, Yougen Tang, and Yadong Li, *Inorg. Chem. Comm*., 2004, 7(6), 731-733.
[26] E.H, Mountstevens , S.A.T. Redfern, J.P. Attfield *Phys Rev B.*, 2005, 71, 220102.
[27] A.L.Patterson, *Phys Rev*., 1939, 56, 978.
[28] K. S. Choi, H.S. Ahn, *J Poly*., 1990, 4, 516-526.
[29] Park Heung Jai, JEONG Seong Wook, YANG jae, Kim Boo Gil, and Lee Seung Mok, *J Environ.Sci*., 2007, 19(12), 1436-1441.
[30] P. Ciambelli, S. Cimino, G. Lasorella, L.Lisi, S. De Rossi, L. Lisi, M. Faticanti, G. Minelli and P. Porta, *Appl. Catal. B & Environ.*, 2002, 37(3), 28 231-241.
[31] Y.Yokoi, and H. Uchida, *Catal. Today*., 1998, 42, 167-174.
[32] M. Machida, K. Eguchi, and H. Arai, *J Catal*.,1989, 120, 377-386.
[33] F.C. Buciuman, F. Patcas, J.C. Menezo, J. Barbier, T. Hahn, and H.G. Lintz, *Appl Catal B Environ.*, 2002, 35,175.
[34] N. Sharma, *Studies on metal oxides as anodes for lithium ion batteries*, Ph.D thesis, ScholarBank @NUS National University of Singapore.
[35] The *Siddha Formulary of India*, Ministry of Health and Family Welfare, Govt. of India, New Delhi, Part I, Hospital Pharmacopoeia 1992.

Received : 9th June, 2013
Revised : 23rd June, 2013
Online : 15th July, 2013